DOI: 10.1002/ ((manuscript number))
Article type: Full Paper

High Performance Pillared Vanadium Oxide Cathode for Lithium Ion Batteries

*Siu on Tung, Krista L. Hawthorne, Yi Ding, James Mainero, and Levi T. Thompson**

S. Tung
Macromolecular Science and Engineering, University of Michigan, Ann Arbor, MI 48109, USA
Dr. K. L. Hawthorne, Prof. L. T. Thompson
Department of Chemical Engineering, University of Michigan, Ann Arbor, MI 48109, USA
E-mail: ltt@umich.edu
Dr. Y. Ding, J. Mainero
U.S. Army, Tank Automotive Research Development and Engineering Center, Warren, MI 48387, USA

Keywords: nanostructured materials, lithium ion batteries, cathode materials, vanadium oxide cathodes, pillared cathode materials

Layered oxides such as $LiCoO_2$ are widely used in the cathodes of lithium ion batteries but their mechanical and thermal properties can lead to safety and reliability (e.g. cycle life) challenges in particular for military vehicle applications. Stresses induced in oxide particles on repeated lithium insertion and extraction, for example, can cause mechanical fracture, a suspected contributor to capacity fade and resistance increases. We hypothesized that the incorporation of pillaring agents between the layers would reduce stresses caused by lithium insertion and enhance lithium diffusion thereby improving cycle-life, high rate capacities and resistance to thermal runaway. This presentation will describe our progress in preparation of the pillared materials, and characterization of their structural, compositional, electrochemical, thermal and mechanical characteristics.

Report Documentation Page

Form Approved
OMB No. 0704-0188

1. REPORT DATE	2. REPORT TYPE	3. DATES COVERED
24 APR 2015		**00-12-2014 to 00-00-2015**

4. TITLE AND SUBTITLE	5a. CONTRACT NUMBER
High Performance Pillared Vanadium Oxide Cathode for Lithium Ion Batteries	5b. GRANT NUMBER
	5c. PROGRAM ELEMENT NUMBER
6. AUTHOR(S)	5d. PROJECT NUMBER
	5e. TASK NUMBER
	5f. WORK UNIT NUMBER
7. PERFORMING ORGANIZATION NAME(S) AND ADDRESS(ES) **US Army RDECOM-TARDEC,6501 E. 11 Mile Road,Warren,MI,48397-5000**	8. PERFORMING ORGANIZATION REPORT NUMBER
9. SPONSORING/MONITORING AGENCY NAME(S) AND ADDRESS(ES)	10. SPONSOR/MONITOR'S ACRONYM(S)
	11. SPONSOR/MONITOR'S REPORT NUMBER(S)

12. DISTRIBUTION/AVAILABILITY STATEMENT
Approved for public release; distribution unlimited

13. SUPPLEMENTARY NOTES
DOI: 10.1002/ ((manuscript number))

14. ABSTRACT
See Report

15. SUBJECT TERMS

16. SECURITY CLASSIFICATION OF:			17. LIMITATION OF ABSTRACT	18. NUMBER OF PAGES	19a. NAME OF RESPONSIBLE PERSON
a. REPORT	b. ABSTRACT	c. THIS PAGE			
unclassified	**unclassified**	**unclassified**	**Same as Report (SAR)**	**14**	

1. Introduction

Due to their relatively high energy densities, rechargeable lithium-ion batteries (LIBs) have enabled a new generation of powerful personal electronics and the arrival of electric vehicles (EVs) and hybrid electric vehicles (HEVs).[1,2] While energy density is a key consideration for batteries used in vehicle applications, the rate capability, cyclability, and safety of LIBs have been identified as critical areas for improvement to allow for the development of reliable, safe, and long lasting battery systems for the next generations of EVs and HEVs.[3] As a result, two major approaches have been taken to increase electrode-electrolyte interfacial area while minimizing lithium diffusion lengths, thereby enhancing the energy and power densities of LIBs: (1) modifying electrode architecture[4] and (2) altering the nanoscale structure of the active electrode material.[5] However, battery safety and life remains to be challenges. The structural stability of active electrode materials is one of a primary drivers of LIB cyclability and safety[6,7] and therefore, high rate capability, cyclability, and safety can be achieved by carefully engineering the nanoscale structure of the electrode materials.

Layered lithium metal oxides are one of the major classes of materials used as cathodes in LIBs. However, despite their wide adoption in batteries for small electronics, these material have not been widely used in vehicle applications due to their relatively poorer structural stability. As an example, lithium cobalt oxide is only stable up to about 170 °C, at which point oxygen liberation is observed.[8] This is especially dangerous in the event of thermal runaway, where the temperature of a battery rises uncontrollably leading to explosion and fire with oxygen and flammable electrolyte solvents acting as fuel.[9] Furthermore, continuous intercalation and de-intercalation of the lithium ions within metal oxide layers during the normal charge and discharge process of a LIB causes mechanical fatigue within the lattice structure.[7] Collapsing layers leads to capacity loss as lithium host sites are lost. In order to

add stability to these layer structured cathode materials, nano-scale pillars inserted between the layers can provide the much needed structural support thus improving thermal and mechanical stability.

Pillaring based on the intercalation of aluminum polyoxocations in two dimensional layered structures has been demonstrated to enhance electrochemical performance[10] and thermal stability[11] of layered materials. With the intercalation of the aluminum polyoxocations, an increase in the interlayer spacing is observed and thus an increase in mesopores and overall surface area.[12] This enhancement in surface area may also have the benefit of exposing more lithium ion accessible area. While complete exfoliation of the these layer materials will yield the maximum surface area and has demonstrated exceptional rate capabilities,[13] the structure integrity of these nanosheets may not be able to withstand prolonged cycling and thermal abuse.

In this work, vanadium pentoxide (V_2O_5) xerogels are selected as a model cathode material to demonstrate the benefits of pillaring in terms of thermal stability, cyclability and rate capability. Despite a high theoretical capacity of up to 562 mAh g^{-1}, V_2O_5 suffers from poor structural stability, slow electrochemical kinetics, and low electronic conductivity.[14] V_2O_5 xerogels and aerogels, in which V_2O_5 layers are swollen with water and subsequently supercritically dried, demonstrates improved kinetics, yet remains susceptible to poor structural stability and thermal stability only up to 300 °C.[15] By taking advantage of the versatile intercalation ability of V_2O_5 xerogels,[16] we insert aluminum polyoxocations between V_2O_5 layers and thus obtain a novel cathode composite material with high rate capability, cyclability, and structural and thermal stability.

2. Materials Characterization

X-ray diffraction was used to determine structure variations between as-made V_2O_5 xerogels (V_2O_5G) and Al_{13} Keggin ion pillared V_2O_5 xerogels (V_2O_5-Al_{13}). V_2O_5 xerogels exhibit a total of 4 diffraction peaks at 7.8, 23.2, 30.8 and 38.7 degrees two-theta, corresponding to its (001), (003), (004), and (005) diffraction planes (**Figure 1**). With the intercalation of the Al_{13} Keggin pillars, the position of the 001 plane shifts to 6.7 degrees two-theta, along with the emergence of two new peaks at 13.2 and 20.0 degrees two-theta (Figure 1(b)). These new peaks are likely the diffraction planes of the added Al_{13} Keggin ions. Additionally, the interlayer spacing of the (001) plane increased from 11.4 Å to 13.2 Å, which matches the reported size of Al_{13} Keggin ions.[17] Elemental analysis using inductively coupled plasma spectroscopy (ICP) shows that 9 wt% aluminum was intercalated into the pillared samples.

In an attempt to observe the stability of the cathode material, Temperature Programmed Desorption (TPD) and Thermal Gravimetric Analysis (TGA) experiments were performed to analyze the water desorption behavior of the V_2O_5G and V_2O_5-Al_{13} samples. At 350 °C, 100% of the water loaded into the V_2O_5 xerogel is removed (**Figure 2 (a) and (c)**). However, in the pillared material only 55% of water loaded in V_2O_5-Al_{13} is removed at 350 °C (Figure 2 (b) and (d)). Pillared V_2O_5 samples dried at 350 ^oC under either air or nitrogen (V_2O_5-Al_{13} 350 °C Air and V_2O_5-Al_{13} 350 °C N_2) were able to maintain their pillared structures, exhibiting similar XRD patterns with the (001) peak position reduced to 6.7 degrees two-theta (Figure 1(c) & (d)). Literature reports that when V_2O_5-Al_{13} samples are dried in either air or nitrogen environments, surface defects are introduced[18] in addition to increased layer spacing. The unpillared V_2O_5 xerogel sample reverted back to crystalline V_2O_5 when dried at 350 °C as expected, with all pillared water molecules removed (Figure S1).

High-resolution transmission electron microscopy (HRTEM) was used to further investigate and visualized the pillared architecture achieved in the V_2O_5G and V_2O_5-Al_{13} samples. HRTEM image of V_2O_5G show a layered nanoribbon structure with lattice spacings of approximately 11.4 Å (**Figure 3 (a)**). This result agrees quite well with the (001) spacing observed in the XRD reported here as well as in previously published results.[19] The interlayer spacing is increased in the case of V_2O_5-Al_{13} as the Al_{13} Keggin ions are intercalated (Figure 3(b)). For V_2O_5-Al_{13} 350 °C Air and V_2O_5-Al_{13} 350 °C N_2 samples (Figure 3(c) & (d)), the observed crystallite sizes are distinctly smaller as the widening XRD peaks have suggested while the interlayer spacing and (001) peak position are still in agreement.

3. Electrochemical Characterization

The V_2O_5G, V_2O_5-Al_{13}, and V_2O_5-Al_{13}-350 °C samples were evaluated electrochemically in coin cells, both through cylic voltammetry and charge/discharge charactarization. The lithium metal anode serves as a quasi Li/Li^+ reference electrode in cyclic voltammetry experiments. Cyclic voltammetry experiments were conducted at 0.1 mV s^{-1} between 2.0 V and 4.0 V versus a Li/Li^+ quasi reference electrode (**Figure 4**). The cyclic voltammetry for the V_2O_5G cell is characteristic of the material,[20,21] with two redox couples observed at 2.6 V and 2.9 V. Pillaring the V_2O_5 xerogel results in a similar cyclic voltammogram, though the redox couple at 2.9 V has much higher peak currents than the redox couple at 2.6 V. Additionally, the decrease in peak separation from the V_2O_5G to the V_2O_5-Al_{13} indicates that the kinetics of lithium ion intercalation was improved with the additions of the Al_{13} Keggin pillars. The improvement in kinetics with pillaring is further exemplified in charge-discharge experiments.

Coin cells containing pillared V_2O_5 materials as the cathode were cycled at varying C rates to examine their retention of capacity, as compared to cells containing the V_2O_5G active material. Cycles were performed at rates of C/10, C/2, C/10, 2C, and C/10, for 10 cycles at each rate. The discharge capacity of each cycle is plotted in Figure 5 with respect to the experimentally observed C/10 capacity of each cell. The V_2O_5G containing cells lost capacity quite quickly, falling to 81% of its initial capacity by the 10^{th} cycle at a rate of C/10. By the 50^{th} cycle, the capacity of the V_2O_5G cell settled at about 60% of its initial capacity at a rate of C/10. All of the pillared materials show increased capacity retention over the V_2O_5 xerogel in the first 10 cycles. Additionally, the cells containing pillared materials retained more of their low rate capacity at higher rates of discharge. The pillared materials treated at 350 °C in nitrogen retained 60% of its low-rate capacity at a rate of C/2, though the untreated pillared V_2O_5 (V_2O_5-Al_{13}) retained more of its initial capacity at cycle 50 (90%).

Long term stability at high rates of discharge is also a concern for Li Ion batteries. The four cathode materials described here were cycled at a rate of C/2 for 100 cycles to investigate their long-term capabilities (Figure 6). Again, the coin cell containing V_2O_5G quickly lost capacity, and settled at around 47 mAh g^{-1}. The cells containing pillared materials both started at higher capacities and maintained a higher capacity throughout cycling. The button cell containing V_2O_5-Al_{13} 350 °C N_2 had a capacity of 102 mAh g^{-1} on the first cycle, and 77 mAh g^{-1} on the 100^{th} cycle. This represents an increase greater than 60% in the long-term capacity over the V_2O_5G cell. The improvement in capacity as well as capacity retention demonstrated in the pillared V_2O_5 xerogels represents a significant improvement over non-pillared V_2O_5 xerogels as alternative cathode materials for Li Ion batteries.

4. Conclusion

Successful pillaring of a V_2O_5 xerogel using Al_{13} Keggin ions was demonstrated through XRD and TEM. Further treatment of the samples at 350 °C in either air or nitrogen showed smaller crystal sizes, while maintaining the layered pillared structure. In electrochemical testing, the pillared V_2O_5 xerogels treated at 350 °C exhibited a significant increase in both capacity and capacity retention over non-pillared V_2O_5 xerogel samples in coin cell testing. Additionally, coin cell cycling with the pillared cathode materials at high rates over a period of 100 cycles showed a higher stability and capacity than in a coin cell with the unpillared V_2O_5.

5. Experimental Section

Xerogel Preparation and Pillaring: To prepare the V_2O_5 xerogel, 3 g of crystalline V_2O_5 powder (Sigma Aldrich, St. Louis, MO) was dissolved in 300 mL of a 10% hydrogen peroxide solution (Fisher Scientific, Waltham, MA) under constant stirring at room temperature. After 18 hours of continuous stirring, the solution was then dried at 50 °C under vacuum overnight to obtain dark red flakes of V_2O_5 xerogel. The flakes were then crushed to obtain a fine V_2O_5 xerogel powder.

Al_{13} Keggin solution was prepared by combining 100 mL of aluminum chloride ($AlCl_3$) and 50 mL of sodium hydroxide (NaOH) in a 2.1:1 molar ratio (both obtained from Sigma Aldrich, St. Louis, MO). The sodium hydroxide solution was added to the $AlCl_3$ solution dropwise, and then aged over 3 days under continuous stirring. Once the Al_{13} Keggin solution was prepared, 2 g of the V_2O_5 xerogel powder were then added to Al_{13} Keggin solution and stirred for 3 days at room temperature to undergo the pillaring process. The pillared V_2O_5 powder was collected using centrifugation and washed repeatedly with de-ionized water. The sample

was then dried under vacuum at 50 °C overnight. Where indicated, samples of the pillared V_2O_5 material were additionally dried at 350 °C under either air or nitrogen for 2 hours.

Materials Characterization: X-ray diffraction (XRD) patterns were obtained using a Rigaku rotating anode X-ray diffractometer. Scanning electron and transmission electron images were obtained using a FEI Nova nanolab SEM/FIB and a JEOL 3011 HREM, respectively.

Electrochemical Measurements: For electrochemical characterization, electrodes were prepared using an ink with a dry composition of 70% active material, 20% Super P Li carbon (TIMCAL, Switzerland), and 10% polyvinylidene fluoride (Kynar, owned by Arkema, Colombes, France) as a binder. The solvent used in the ink was n-methyl pyrrolidone (Sigma-Aldrich, St. Louis, MO). A high-speed mixer obtained from FlakTech (Landrum, SC) was used to ensure the ink was well mixed. The ink was doctor bladed on a clean aluminum foil current collector, then dried for two hours under air at 110 °C, then under vacuum at 110 °C overnight. Active material loading was determined by the weight after drying.

Cyclic voltammetry, capacity, and charge/discharge measurement were performed using 2032 coin cells assembled in an argon filled glovebox. Lithium metal discs obtained from XX (from XX) were used as the anode, with a Celgard 2500 separator (Celgard, Charlotte, NC). The electrolyte was a commercially available mixture of ethylene carbonate and dimethyl carbonate (1:1 v/v) with 1 M $LiPF_6$ as the supporting electrolyte, obtained from SoulBrain (XX). Galvanostatic charge-discharge experiments were done with a Maccor Series 4000 multichannel battery test stand. Cyclic voltammetry was done using a Metrohm Autolab potentiostat, with the lithium metal counter electrode serving as a Li/Li^+ quasi reference electrode.

Supporting Information ((delete if not applicable))
Supporting Information is available from the Wiley Online Library or from the author.

Acknowledgements
((Acknowledgements, general annotations, funding. Other references to the title/authors can also appear here, such as "Author 1 and Author 2 contributed equally to this work."))

Received: ((will be filled in by the editorial staff))
Revised: ((will be filled in by the editorial staff))
Published online: ((will be filled in by the editorial staff))

[1] B. Dunn, H. Kamath, J. Tarascon, *Science* **2011**, *334*, 928.

[2] M. Armand, J. Tarascon, *Nature* **2008**, *451*, 652.

[3] C. M. Hayner, X. Zhao, H. H. Kung, *Annu. Rev. Chem. Biomol. Eng.* **2012**, *3*, 445.

[4] H. Zhang, X. Yu, P. V. Braun, *Nature Nanotechnology* **2011**, *6*, 277.

[5] K. Kang, Y. Meng, J. Bréger, C. Grey, G. Ceder, S*cience* **2006**, *311*, 977.

[6] J. W. Fergus, *J. Power Sources* **2010**, *195*, 939.

[7] J. Vetter, P. Novák, M. R. Wagner, C. Veit, K.-C. Möller, J. O. Besenhard, M. Winter, M. Wohlfahrt-Mehrens, C. Vogler, A. Hammouche, *J. Power Sources* **2005**, *147*, 269.

[8] Y. Baba, S. Okada, J. Yamaki, *Solid State Ionics* **2002**, *148*, 311.

[9] Q. Wang, P. Ping, X. Zhao, G. Chu, J. Sun, C. Chen, *J. Power Sources* **2012**, *208*, 210.

[10] D. Petridis, P. S. de Kaviratna, T. J. Pinnavaia, *J. Electroanal. Chem.* **1996**, *410*, 93. (1996).

[11] S. M. Thomas, M. L. Occelli, *Clays and Clay Minerals* **2000**, *48*, 304.

[12] L. Wang, Y. Ebina, K. Takada, K. Kurashima, *Adv. Mater.* **2004**, *16*, 1412.

[13] Q. An, Q. Wei, L. Mai, J. Fei, X. Xu, Y. Zhao, M. Yan, P. Zhang, S. Huang, *Phys. Chem. Chem. Phys.* **2013**, *38*, 16828.

[14] M. S. Whittingham, *Chem. Rev.* **2004**, *104*, 4271.

[15] A. Pan, J.-G. Zhang, Z. Nie, G. Cao, B. W. Arey, G. Li, S. Liang, J. Liu, *J. Mater. Chem.* **2010**, *20*, 9193.

[16] G. S. Zakharova, V. L. Volkov, *Russ. Chem. Rev.* **2003**, *72*, 311

[17] W. Casey, *Chem. Rev.* **2006**, *106*, 1.

[18] D. Liu, Y. Liu, A. Pan, K. P. Nagle, G. T. Seidler, Y.-H. Jeong, G. Cao, *J. Phys. Chem.* **2011**, *115*, 4959

[19] V. Petkov, P. N. Trikalitis, E. S. Bozin, S. J. L. illinge, T. Vogt, M. G. Kanatzidis, *J. Am. Chem. Soc.* **2002**, *124*, 10157.

[20] S. Mège, Y. Levieux, F. Ansart, J. M. Savriault, A. Rousset, *J. App. Electrochem.*. **2000**, *30*, 657.

[21] Y. Wang, H. Shang, T. Chou, G. Cao, *J. Phys. Chem.*, **2005**, *109*, 11361.

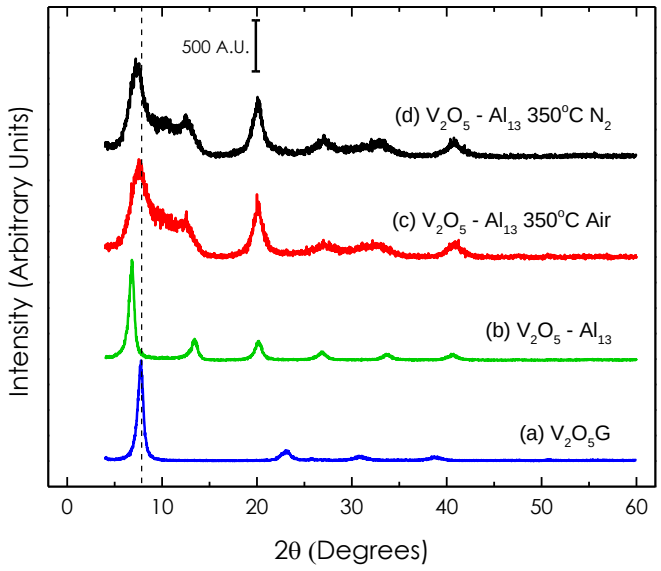

Figure 1. X-ray Diffraction patterns of (a) V_2O_5 xerogel, (b) Al_{13} Keggin intercalated V_2O_5 xerogel, (c) Al_{13} Keggin intercalated V_2O_5 xerogel dried in atomspheric environment at 350 °C, and (d) Al_{13} Keggin intercalated V_2O_5 xerogel dried in nitrogen environment at 350 °C. The dotted line is intended as a guide for the eye.

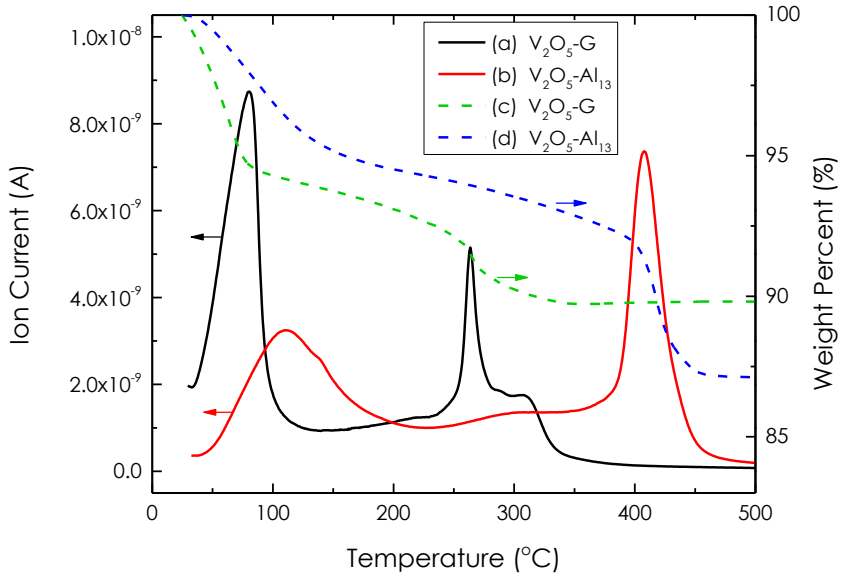

Figure 2. Water (18 g mol^{-1}) ion current of temperature programmed desorption experiment of (a) V_2O_5 xerogel, (b) Al_{13} Keggin intercalated V_2O_5 xerogel. Thermal gravimetric analysis of (c) V_2O_5 xerogel, (d) Al_{13} Keggin intercalated V_2O_5 xerogel.

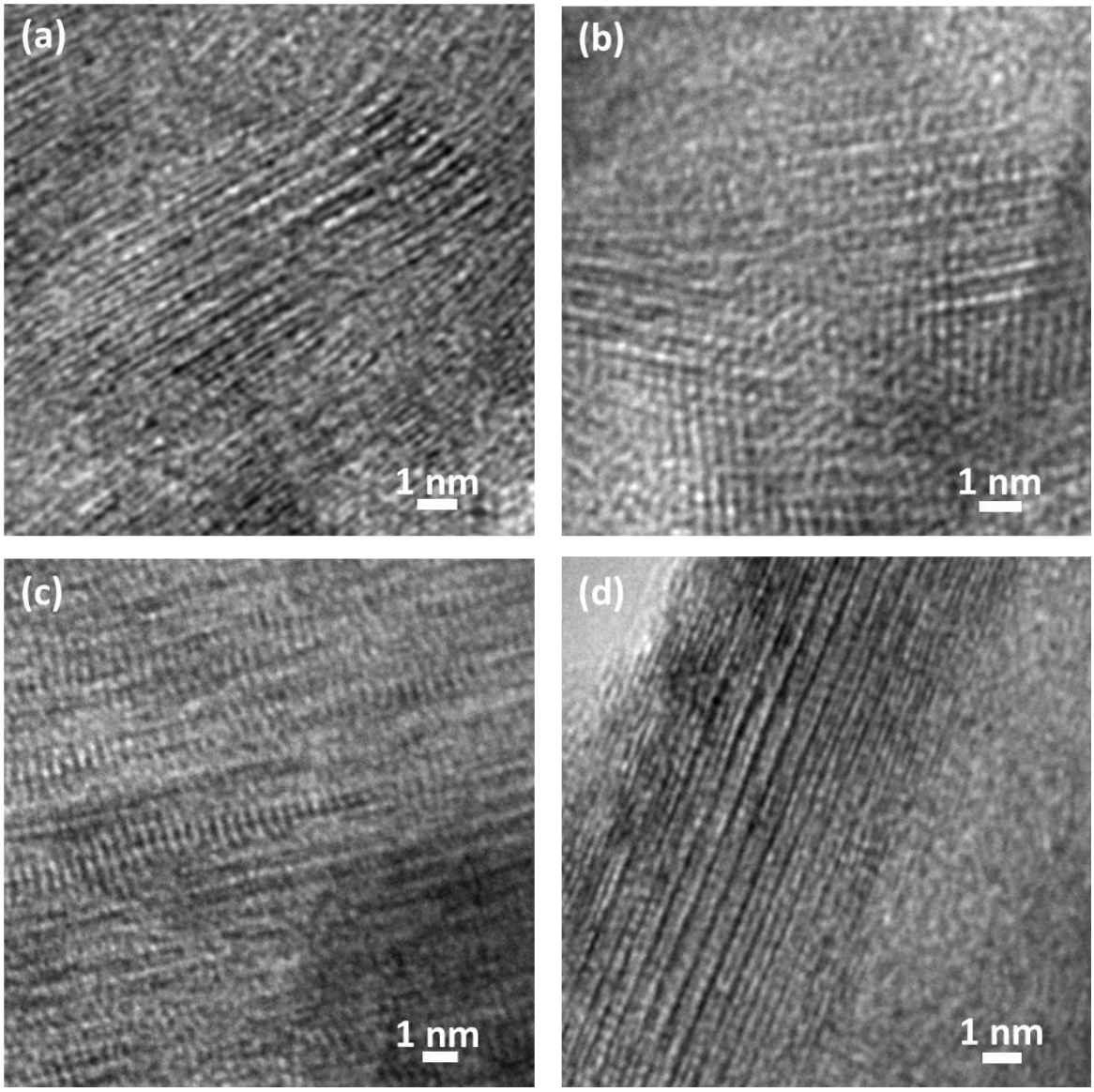

Figure 3. Representative high-resolution transmission electron micrographs of (a) V_2O_5 xerogel, (b) Al_{13} Keggin intercalated V_2O_5 xerogel, (c) Al_{13} Keggin intercalated V_2O_5 xerogel dried in atomspheric environment at 350 °C, and (d) Al_{13} Keggin intercalated V_2O_5 xerogel dried in nitrogen environment at 350 °C.

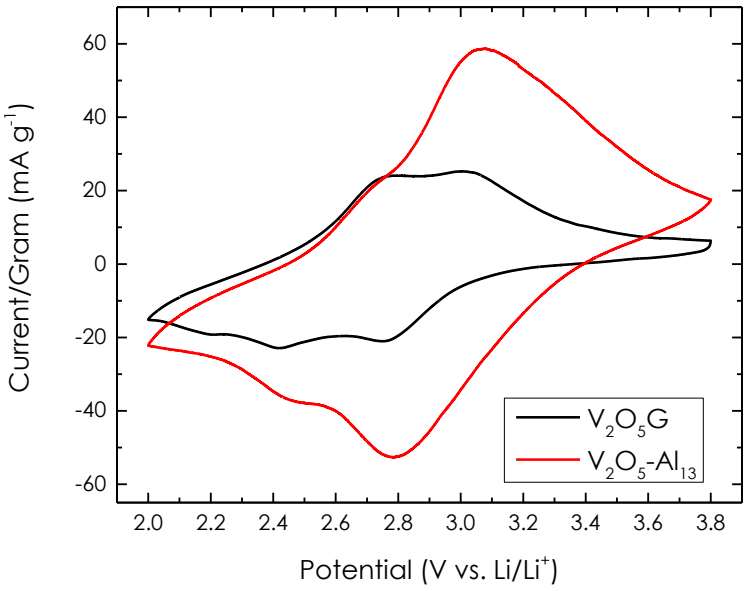

Figure 4. Cyclic voltammetry of Li intercalation in V_2O_5G and V_2O_5-Al_{13} cathode materials. Cycled at 0.1 mV s^{-1}.

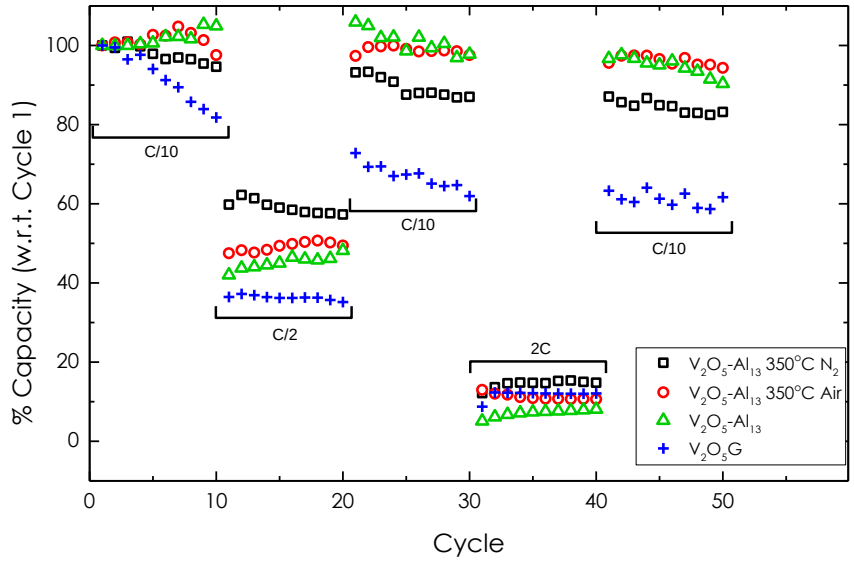

Figure 5. Discharge capacity with respect to the C/10 capacity of each cell for button cells containing V_2O_5G, V_2O_5-Al_{13}, and V_2O_5-Al_{13} treated at 350 °C in either air or nitrogen as the cathode material. Cycles were performed at rates of C/10, C/2, C/10, 2C, and C/10 for 10 cycles each.

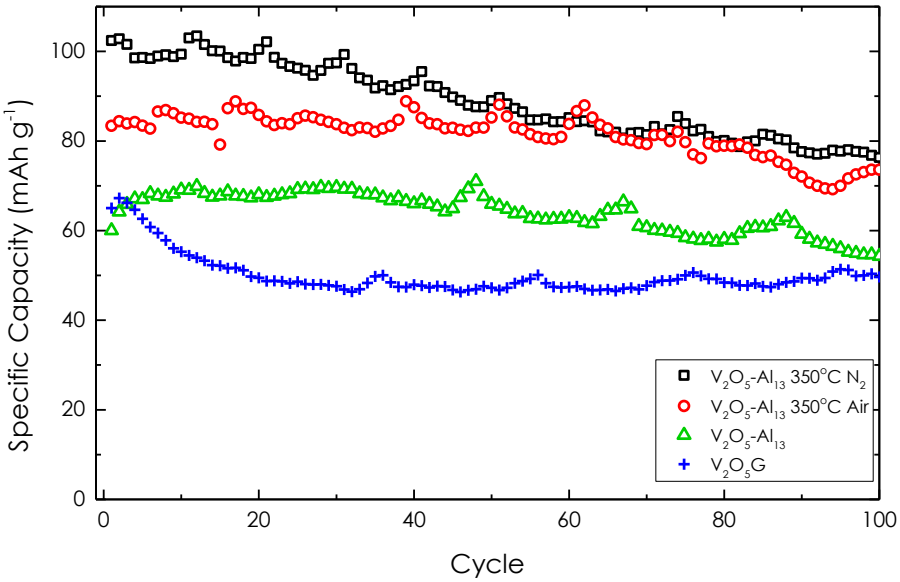

Figure 6. Specific capacity of button cells containing cathodes made of pillared V_2O_5 materials, as compared to the V_2O_5 xerogel (V_2O_5G), over long-term cycling. Cycles were performed at a rate of C/2, for 100 cycles.